SSNV246 - Application of a pressure distributed on the lips of a crack XFEM with the facets of contact resulting from under elements from integration

Summary:

It is about a test of validation of the facets of contact resulting from under elements from integration XFEM.

The facets of contact used by default do not result from under elements from integration and do not give the possibility of having quadratic facets of contact in 3D. One can activate the recovery of the facets of contact resulting from under elements from integration in the operator MODI_MODELE_XFEM with the keyword DECOUPE_FACETTE=' SOUS_ELEMENTS'. One then has linear and quadratic facets in 2D as in 3D which have the advantage of being in conformity with under elements of integration since they are selected among the sides of under elements of integration in 2D and the faces of under elements of integration in 3D. This mode of recovery also has the following advantage: the coordinates of the nodes of these facets are not recomputed as it is the case by default, because these nodes are recovered during the cutting which is carried out in TOPOSE.

In this test, one makes sure of the good performance of the recovery of these facets when a mechanical pressure is applied to the lips of the crack. Different geometries are proposed in 2D and in 3D, the got results are compared with an analytical solution. One voluntarily chooses an Iso-zero “lsn curve” representing the interface in the geometry 2D and the geometry 3D to appreciate the performance profit brought by the quadratic “facetisation”.

1 Problem of reference

1.1 Geometry of the problem 2D (modelings A and B)

It is about a square on side $L=10\,m$. This bar has a discontinuity of the type interfaces (interface nonwith a grid which is introduced into the model via the level-sets thanks to the operator DEFI_FISS_XFEM). The square is thus entirely crossed by discontinuity (on the level of the approximation of the field of displacements, one takes into account only Heaviside enrichment). Discontinuity is circular of center $O(0,-2)$ and of ray $R=9\,m$.

One represents on the Figure 1.1-a geometry of the problem.

Figure 1.1-a: Geometry of the problem 2D

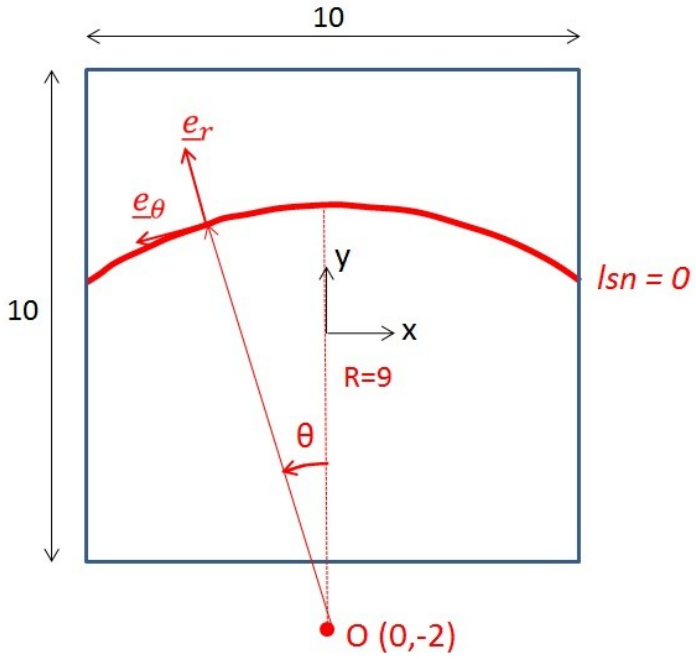

1.2 Geometry of the 3D problem (modelings C and D)

It is about a eighth of sphere of interior ray $R_i=1\,m$, of external ray $R_e=2\,m$ and of cente $O(0,0,0)$. This portion of sphere is crossed by a discontinuity of the type interfaces (interface nonwith a grid which is introduced into the model via the level-sets thanks to the operator DEFI_FISS_XFEM), concentric of ray $R=1.5\mathrm{m}$.

One represents on the Figure 3.2-a geometry of the column.

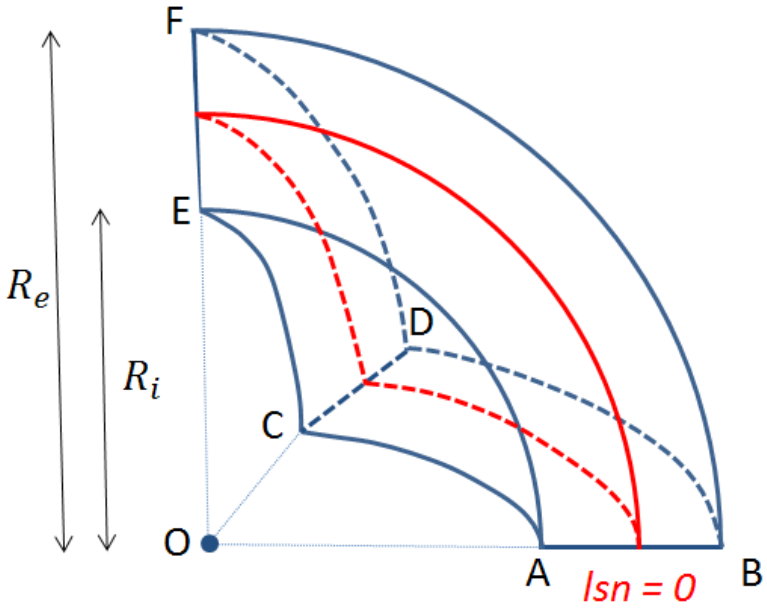

1.3 Properties materials

Parameters given in the Table 1.3-1 , correspond to the parameters used for 4 modelings. The behavior is elastic ('ELAS').

Elastic parameters	Young modulus $E(en\,MPa)$	5800
	Poisson's ratio ν	0
	Thermal dilation coefficient $\alpha(en\,K^{-1})$	0

Table 1.3-1 : Properties of material

1.4 Boundary conditions and loading

Case 2D

The following conditions of Dirichlet are applied:

- on the lower side of the square, displacements are blocked in all the directions ($u_x=0$ and $u_y=0$),
- on the higher side of the square, displacements according to x are blocked $u_x=0$ and one imposes a crushing of the following square y , $u_y=u_{y,\,impo}=-1.E^{-6}$.

One applies in the crack "the pressure and the shearing of contact". I.e. that the efforts are applied that there would be on the level of the crack if the square were not fissured where if there were a perfect adherent contact. The conditions of Neuman are thus the following ones:

- on each lip of the interface one imposes a pressure distributed $p(\theta)=\sigma_{yy}*cos^2(\theta)$ via AFFE_CHAR_MECA and of the keyword CRACK of PRES_REP .

- on each lip of the interface one imposes a shearing distributed $t(\theta)=-\sigma_{yy}*\cos(\theta)\sin(\theta)$ via AFFE_CHAR_MECA and of the keyword CRACK of CISA_2D .

Case 3D

The following conditions of Dirichlet are applied:

- on the lower face [ABDC], displacements according to z are blocked $u_z=0$,
- on face [ABFE], displacements according to y are blocked $u_y=0$,
- on face [CDFE], displacements according to x are blocked $u_x=0$,
- on the external cap BDF and the interior cap ACE, displacements are blocked in all the directions ($u_x=0$, $u_y=0$ and $u_z=0$).

The loading is the following:

- on each lip of the interface with $r=R$ a pressure distributed uniform is imposed $p=10\,MPa$ via AFFE_CHAR_MECA and of the keyword CRACK of PRES_REP.

2 Reference solution

2.1 Method of calculating

In the case 2D and the case 3D, it is about an analytical solution. Taking into account the boundary conditions, displacements can be obtained starting from the analytical resolution of the conservation equation of the momentum.

Case 2D

The Poisson's ratio ν being null, the problem is unidimensional according to y . The tensor of the constraints is uniform in all the field: $\boldsymbol{\sigma}=E\,\boldsymbol{\epsilon}=E*\epsilon_{yy}\boldsymbol{e}_y\otimes\boldsymbol{e}_y$.

However $\mathbf{Div}(\boldsymbol{\sigma})=\mathbf{0}$ thus $\frac{\partial\epsilon_{yy}}{\partial y}=0$. According to the boundary conditions applied $\epsilon_{yy}=\frac{u_{\text{y, impo}}}{L}$

Finally, $\boldsymbol{\sigma}=E*\frac{u_{\text{y, impo}}}{L}\boldsymbol{e}_y\otimes\boldsymbol{e}_y=\sigma_{yy}\boldsymbol{e}_y\otimes\boldsymbol{e}_y$.

On the level of the crack, $e_r=-\sin(\theta)\boldsymbol{e}_{\mathbf{x}}+\cos(\theta)\boldsymbol{e}_{\mathbf{y}}$ and $e_\theta=-\cos(\theta)\boldsymbol{e}_{\mathbf{x}}-\sin(\theta)\boldsymbol{e}_{\mathbf{y}}$.

On the level of a point of the crack of coordinates (R,θ) , if there were no crack, one would have:

$$\boldsymbol{\sigma}.\boldsymbol{e}_{\mathbf{r}}=(\boldsymbol{e}_{\mathbf{r}}.\boldsymbol{\sigma}.\boldsymbol{e}_{\mathbf{r}})\boldsymbol{e}_{\mathbf{r}}+(\boldsymbol{e}_{\mathbf{r}}.\boldsymbol{\sigma}.\boldsymbol{e}_{\boldsymbol{\theta}})\boldsymbol{e}_{\boldsymbol{\theta}}=\sigma_{yy}*[(\boldsymbol{e}_y.\boldsymbol{e}_r)^2\boldsymbol{e}_{\mathbf{r}}+(\boldsymbol{e}_y.\boldsymbol{e}_r)x(\boldsymbol{e}_y.\boldsymbol{e}_{\boldsymbol{\theta}})\boldsymbol{e}_{\boldsymbol{\theta}}]$$

$$\boldsymbol{\sigma}.\boldsymbol{e}_{\mathbf{r}}=\sigma_{yy}*(cos^2(\theta)\boldsymbol{e}_{\mathbf{r}}-\sin(\theta)\cos(\theta)\boldsymbol{e}_{\boldsymbol{\theta}})$$

Finally the solution of the problem is:

$$\boldsymbol{\sigma}=\sigma_{yy}\boldsymbol{e}_y\otimes\boldsymbol{e}_y$$

$$\boldsymbol{u}(x,y)=\frac{u_{\text{y, impo}}}{L}*(\frac{L}{2}+y)$$

Case 3D

By neglecting gravity, the equation is written (in total constraints):

$$\mathbf{Div}(\boldsymbol{\sigma})=\mathbf{0}$$

The Fish module ν being null, and being in the elastic case, one has $\boldsymbol{\sigma}=E\,\boldsymbol{\epsilon}$.

The volume studied with spherical symmetry, consists of a homogeneous and isotropic material; the boundary conditions have also spherical symmetry. One is thus brought to seek a solution of the problem in a spherical frame of reference (r,θ,φ) such as the fields of displacement, of constraint and deformation are respectively of the form:

$$\begin{cases} u_r=h(r) \\ u_\theta=u_\varphi=0 \end{cases} \qquad \begin{cases} \sigma_{rr}=f_1(r) \\ \sigma_{\theta\theta}=\sigma_{\varphi\varphi}=g_1(r) \\ \sigma_{r\theta}=\sigma_{r\varphi}=\sigma_{\theta\varphi}=0 \end{cases} \qquad \begin{cases} \epsilon_{rr}=f_2(r) \\ \epsilon_{\theta\theta}=\epsilon_{\varphi\varphi}=g_2(r) \\ \epsilon_{r\theta}=\epsilon_{r\varphi}=\epsilon_{\theta\varphi}=0 \end{cases}$$

The equilibrium equation $\mathbf{Div}(\boldsymbol{\sigma})=\mathbf{0}$ is reduced then to: $\frac{d\sigma_{rr}}{dr}+\frac{2}{r}*(\sigma_{rr}-\sigma_{\theta\theta})=0$

The boundary conditions static are form: $\sigma_{rr}(R)=-p$

The equations kinematics have the form: $\begin{cases}\epsilon_{rr}=\frac{du_r}{dr}\\ \epsilon_{\theta\theta}=\frac{u_r}{r}\end{cases}$ that is to say finally: $\begin{cases}\sigma_{rr}=E*\frac{du_r}{dr}\\ \sigma_{\theta\theta}=E*\frac{u_r}{r}\end{cases}$

In substituent these two relations in the equilibrium equation one obtains:

$$\frac{d^2u_r}{dr^2}+\frac{2}{r}*(\frac{du_r}{dr}-\frac{u_r}{r})=0 \quad \text{that is to say} \quad \frac{d}{dr}(\frac{1}{r^2}\frac{d(r^2u_r)}{dr})=0$$

The solution of this differential equation is: $u_r(r)=C_1r+\frac{C_2}{r^2}$. The solution sought being discontinuous in R, one separately solves this equation on the two fields $[R_i,R]$ and $[R,R_e]$.

Finally: $\begin{cases}u_r(r)=C_1r+\frac{C_2}{r^2} & sur\,[R_i,R]\\ u_r(r)=C_3r+\frac{C_4}{r^2} & sur\,[R,R_e]\end{cases}$

According to the boundary conditions kinematics, $u_r(R_i)=u_r(R_e)=0$ thus $\begin{cases}C_1R_i+\frac{C_2}{R_i^2}=0\\ C_3R_e+\frac{C_4}{R_e^2}=0\end{cases}$

In addition $\sigma_{rr}=E*\frac{du_r}{dr}=\begin{cases}E*C_1-2E*\frac{C_2}{r^3} & sur\,[R_i,R]\\ E*C_3-2E*\frac{C_4}{r^3} & sur\,[R,R_e]\end{cases}$ thus according to the boundary conditions static: $\begin{cases}C_1-2*\frac{C_2}{R^3}=-\frac{p}{E}\\ C_3-2*\frac{C_4}{R^3}=-\frac{p}{E}\end{cases}$.

The resolution of the system gives

$$\begin{cases} C_1 = \dfrac{-p}{E*\left(2*\dfrac{R_i^{\,3}}{R^3}+1\right)} \\ C_2 = \dfrac{p}{E*\left(\dfrac{2}{R^3}+\dfrac{1}{R_i^{\,3}}\right)} \\ C_3 = \dfrac{-p}{E*\left(2*\dfrac{R_e^{\,3}}{R^3}+1\right)} \\ C_4 = \dfrac{p}{E*\left(\dfrac{2}{R^3}+\dfrac{1}{R_e^{\,3}}\right)} \end{cases}$$

2.2 Sizes and results of reference

To supplement.

2.3 Uncertainties on the solution

No, the solution is analytical.

3 Modeling A

3.1 Characteristics of modeling

It is about a modeling D_PLAN using linear elements HM-XFEM.

3.2 Characteristics of the grid

The square on which one carries out modeling is divided into 16 QUAD4. The interface is nonwith a grid and cuts the square horizontally. The grid is represented Figure 3.2-a.

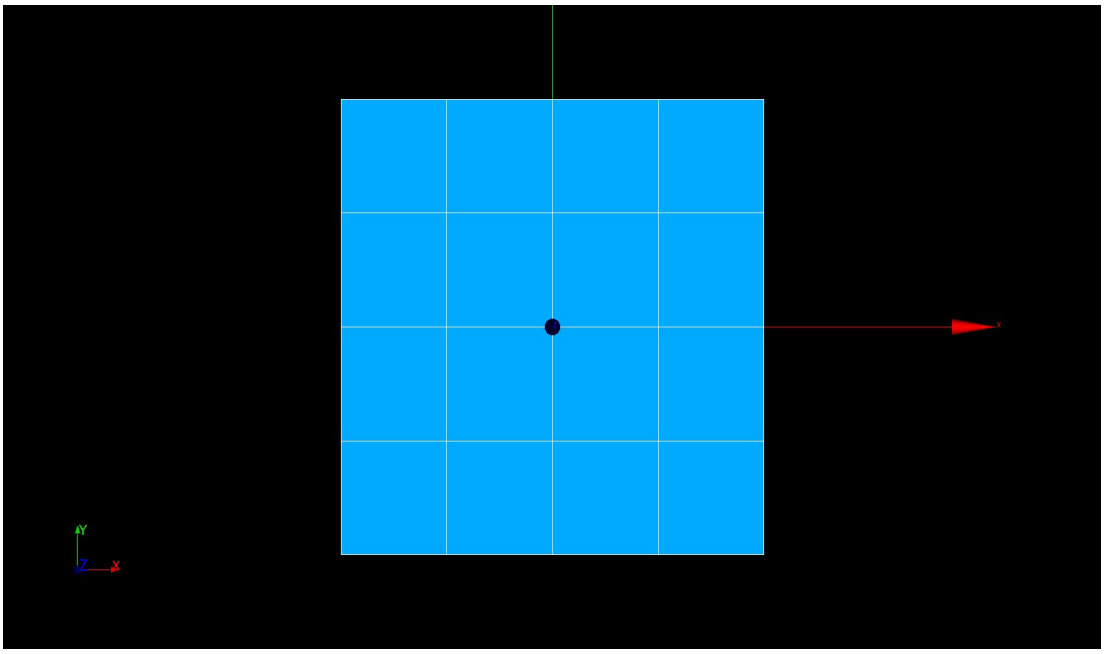

Figure 3.2-a: Grid 2D

3.3 Sizes tested and results

The results are got with *Code_Aster* (resolution with STAT_NON_LINE). The horizontal constraint is tested σ_{xx} supposed uniformly worthless and the vertical constraint σ_{yy} presumedly uniform of value $-E$. With this intention, it is tested MIN and it MAX of these two sizes in all the element. The got results are synthesized in the table below.

Sizes tested	Type of reference	Values of reference	Tolerance
SIGMAXX (MPa) MIN	'ANALYTICAL'	0.0	30
SIGMAXX (MPa) MAX	'ANALYTICAL'	0.0	45
SIGMAYY (MPa) MIN	'ANALYTICAL'	-5800.0	8 %
SIGMAYY (MPa) MAX	'ANALYTICAL'	-5800.0	4 %

Displacements according to y and the deformation are represented on the Figure 3.3-a. One observes well a linear compression of the square, little disturbed by the presence of the crack.

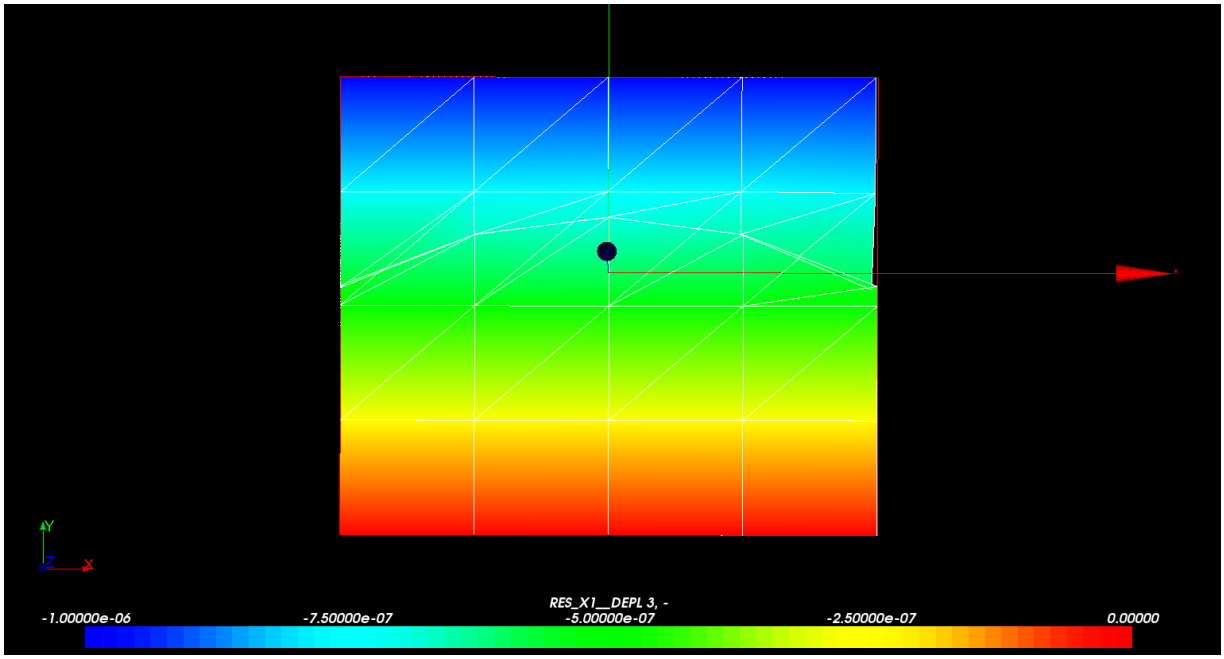

Figure 3.3-a: Field of displacements according to direction (OY)

On the other hand, on the Figures 3.3-b and 3.3-c, one observes the variations of the stress field compared to the analytical solution, in particular in the vicinity of the crack and near as of edges. The relative precision obtained can appear poor but it should be put in relation to the low number of elements used and the important curve of discontinuity.

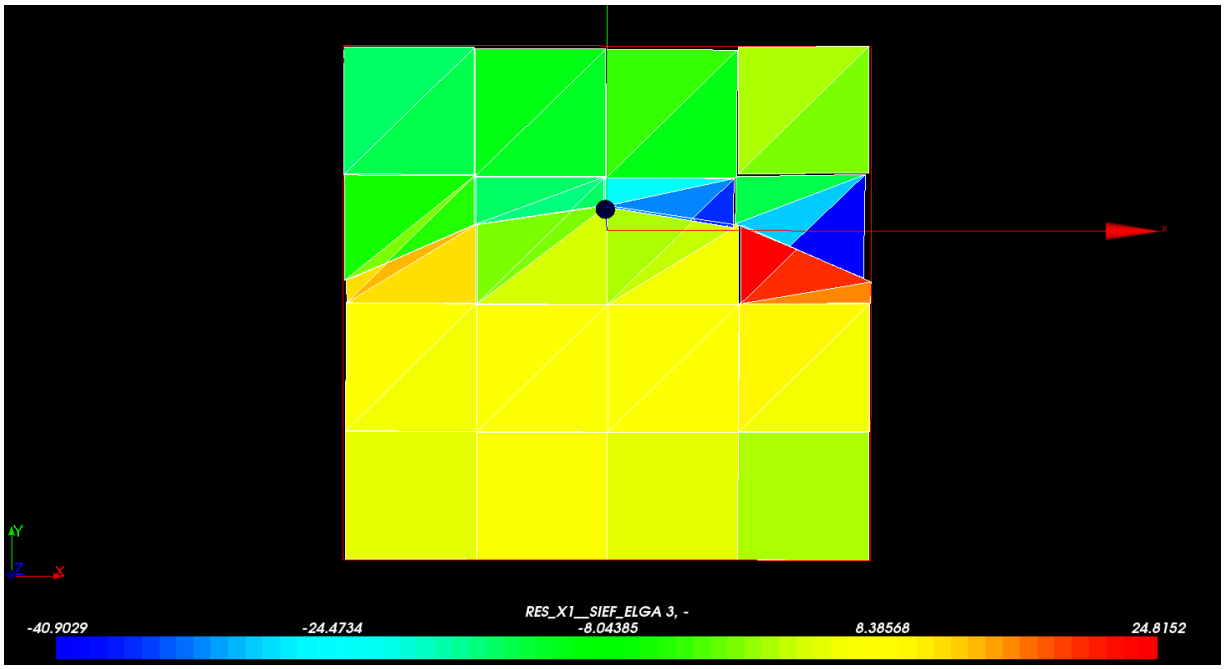

Figure 3.3-b: Stress field σ_{xx}

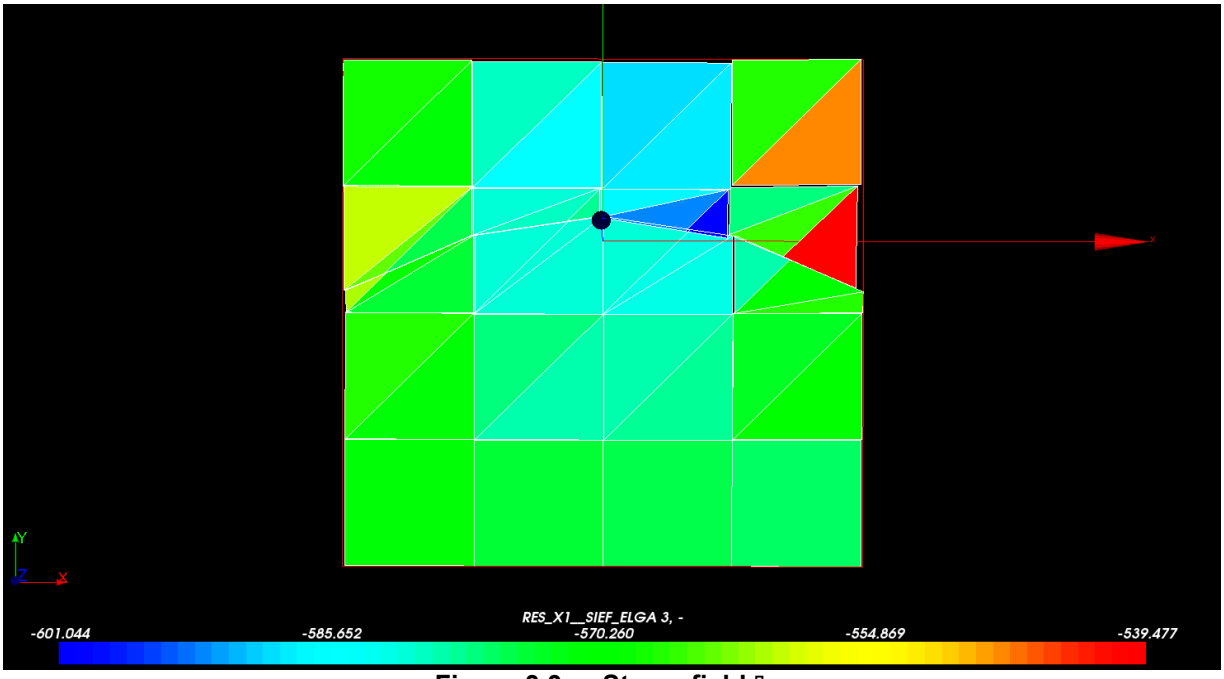

Figure 3.3-c: Stress field σ_{yy}

4 Modeling B

4.1 Characteristics of modeling

This modeling is strictly identical to the preceding one, except for the elements used which are quadratic.

4.2 Characteristics of the grid

The square on which one carries out modeling is divided into 16 QUAD8. The interface is nonwith a grid and cuts the square horizontally.

4.3 Sizes tested and results

The results are got with *Code_Aster* (resolution with STAT_NON_LINE). The horizontal constraint is tested σ_{xx} supposed uniformly worthless and the vertical constraint σ_{yy} presumedly uniform of value $-E$. With this intention, it is tested MIN and it MAX of these two sizes in all the element. The got results are synthesized in the table below.

Sizes tested	Type of reference	Values of reference	Tolerance
SIGMAXX (MPa) MIN	'ANALYTICAL'	0.0	0.01
SIGMAXX (MPa) MAX	'ANALYTICAL'	0.0	0.02
SIGMAYY (MPa) MIN	'ANALYTICAL'	-5800.0	0,002 %
SIGMAYY (MPa) MAX	'ANALYTICAL'	-5800.0	0,001 %

Displacements according to y and the deformation are represented on the Figure 4.3-a. One observes well a linear compression of the square, which is carried out as if the crack were not present.

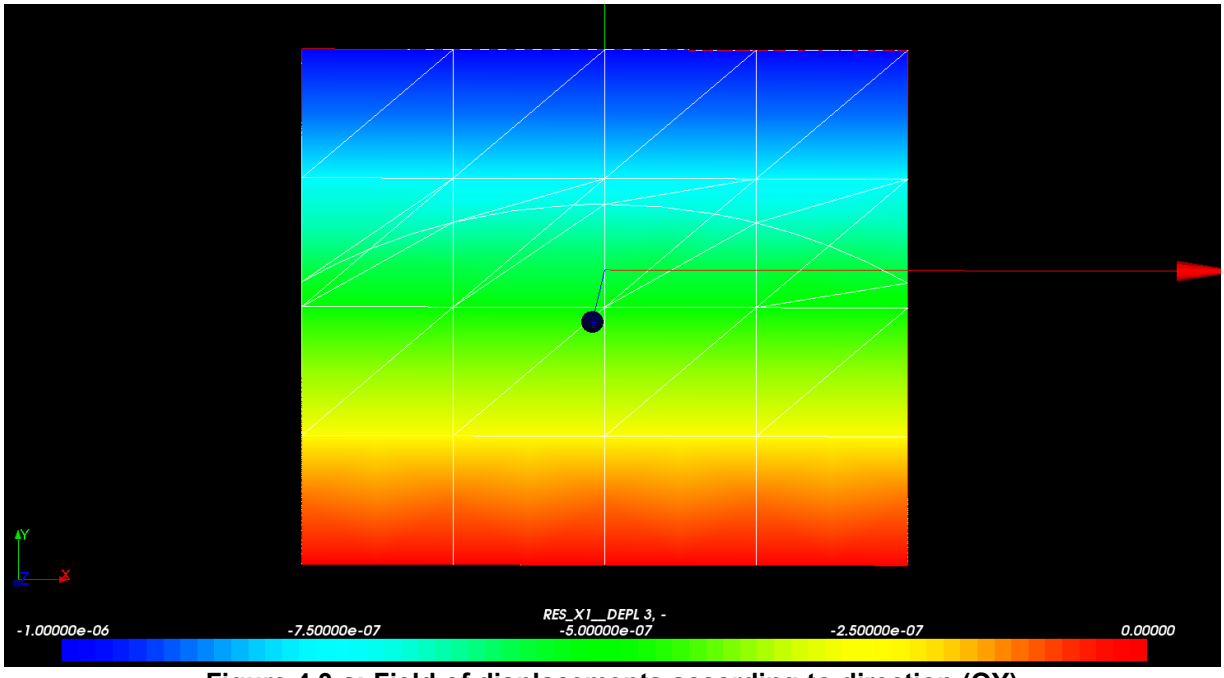

Figure 4.3-a: Field of displacements according to direction (OY)

On the Figures 4.3-b and 4.3-c, it is confirmed that the variations in constraints compared to the analytical solution are reduced in a consequent way compared to preceding linear modeling. The

relative error decreases by a factor 10^5 . Very light variations are always observed in the vicinity of the crack and the level of the edges.

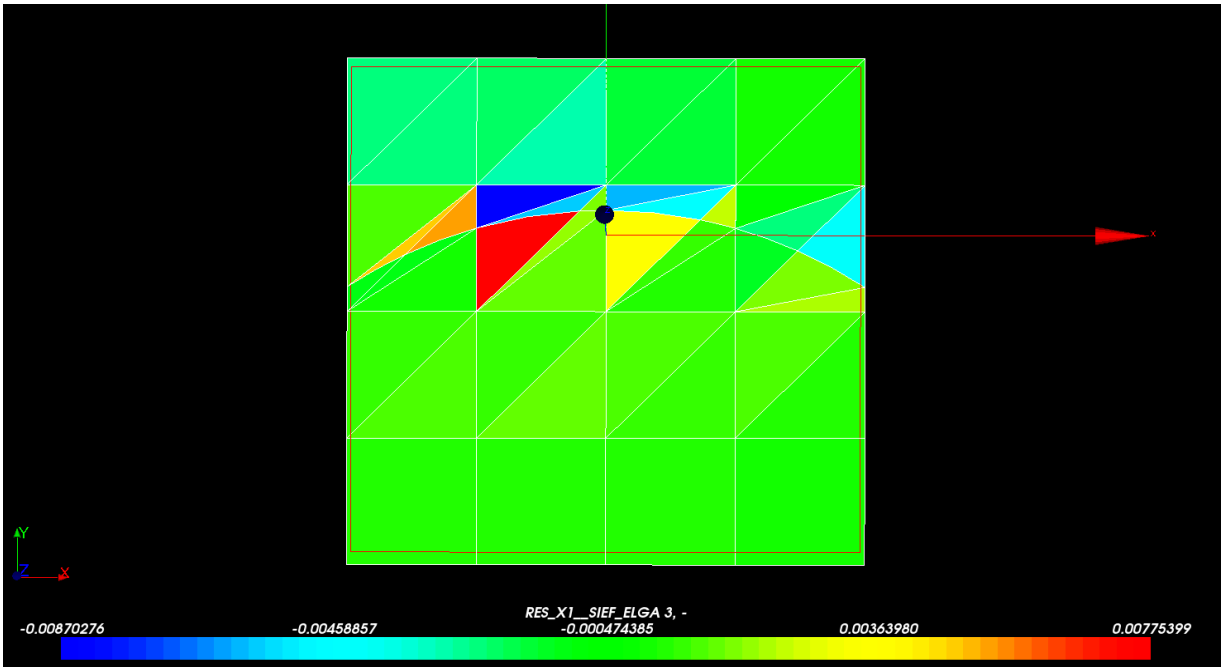

Figure 4.3-b: Stress field σ_{xx}

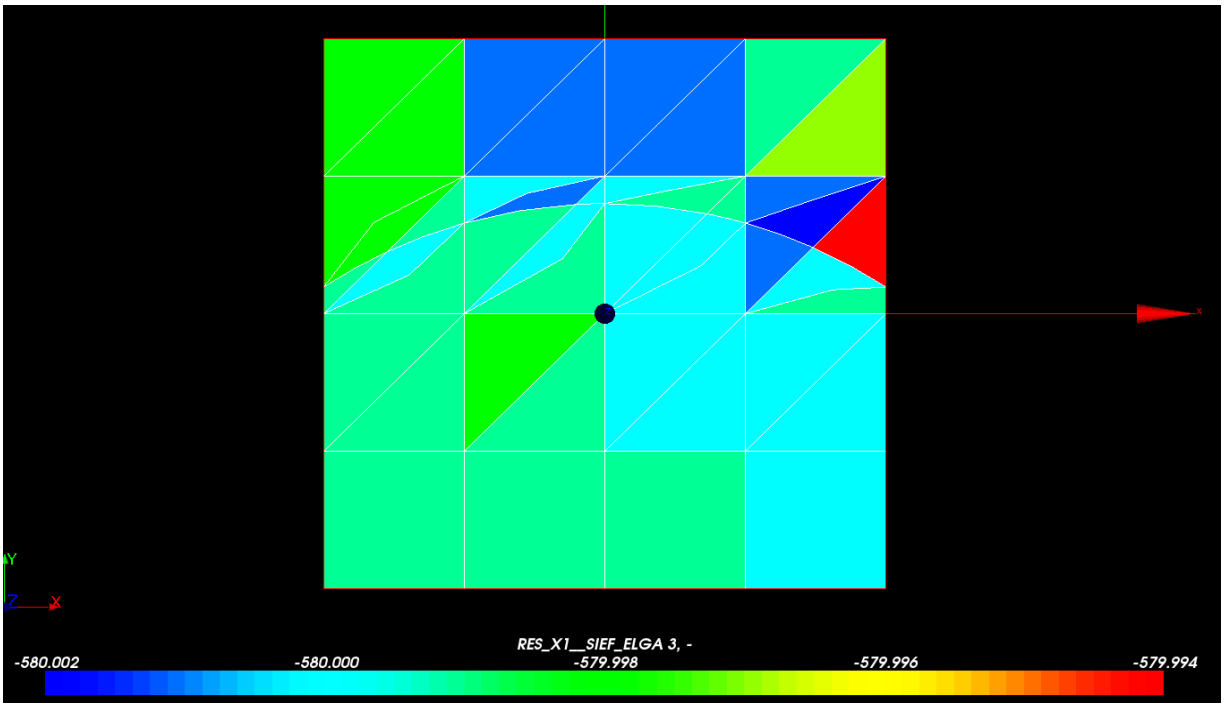

Figure 4.3-c: Stress field σ_{yy}

Two preceding modelings validate the use of the facets of contact resulting from under elements from integration for the application from a mechanical pressure and a shearing on the lips from crack for modelings 2D, linear and quadratic. One notes in particular the important profit in precision when quadratic elements are used. Even if discontinuity is curved, one obtains an excellent precision with very few elements.

5 Modeling C

5.1 Characteristics of modeling

It is about a modeling 3D using linear elements XFEM.

5.2 Characteristics of the grid

The segment of a sphere on which one carries out modeling is divided into 18 HEXA8 and 9 PENTA6. The interface is nonwith a grid and cuts the cap in its thickness. The grid is represented Figure 5.2-a.

Figure 5.2-a: Linear grid 3D

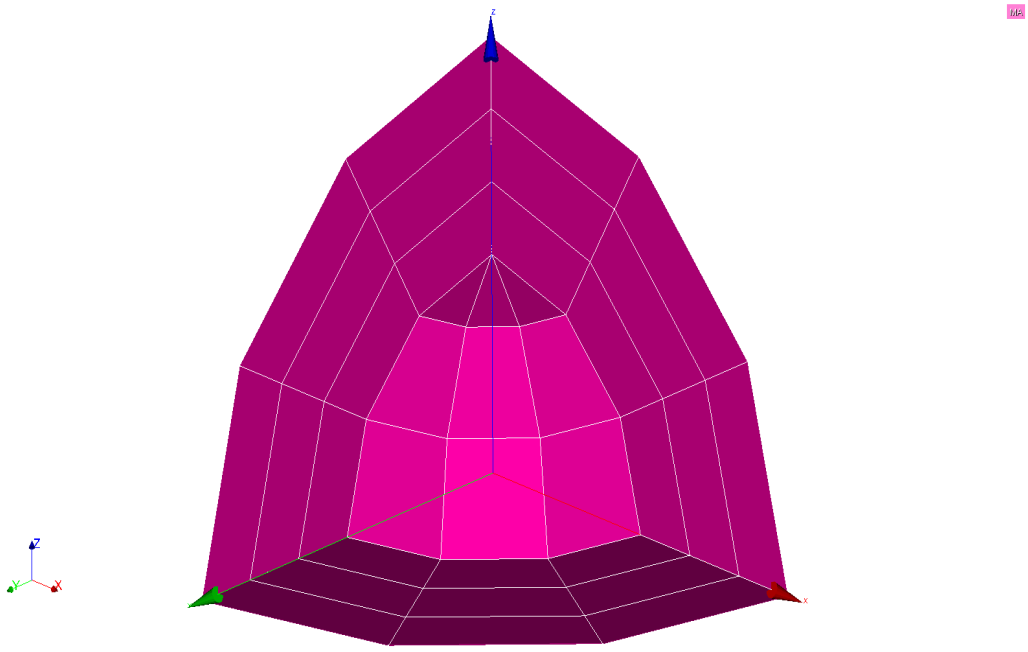

5.3 Sizes tested and results

The results are got with *Code_Aster* (resolution with STAT_NON_LINE). Radial displacements are tested u_r on the lips of the crack. For each crack, it is tested MIN and it MAX of these two sizes for all the nodes of the crack. The got results are synthesized in the table below.

Sizes tested	Type of reference	Analytical values	Tolerance (%)
DR. (int) MIN	'ANALYTICAL'	-0.0001142742582	10.
DR. (int) MAX	'ANALYTICAL'	-0.0001142742582	10.
DR. (ext.) MIN	'ANALYTICAL'	6.173526141E-05	10.
DR. (ext.) MAX	'ANALYTICAL'	6.173526141E-05	10.

Radial displacement u_r and the deformation are represented on the Figure 5.3-a. One observes a clear discontinuity of displacements and the spherical symmetry of the fields.

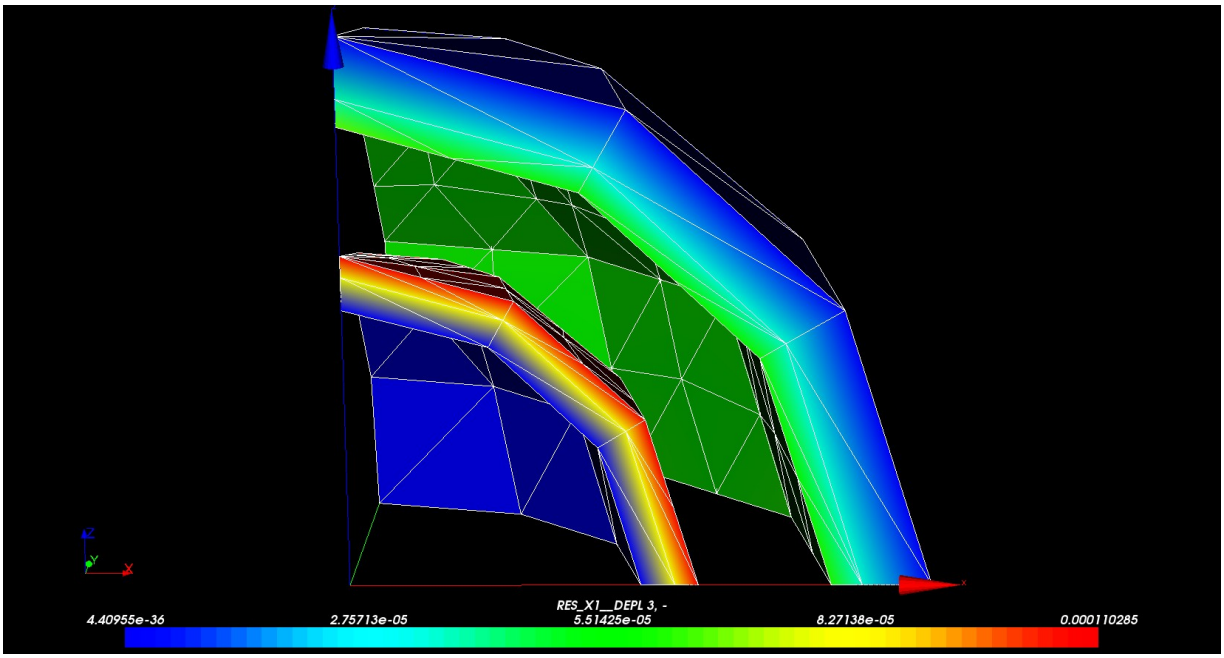

Figure 5.3-a: Field of radial displacement

The variations noted with the analytical solution are to be put in prospect with poverty for the grid used. One uses only 3 meshs in the thickness of the cap and the longitudinal and southernmost directions.

6 Modeling D

6.1 Characteristics of modeling

This modeling is strictly identical to the preceding one, except for the elements used which are quadratic.

6.2 Characteristics of the grid

The cap on which one carries out modeling is divided into 18 HEXA20 and 9 PENTA15. The interface is nonwith a grid and cuts the cap in its thickness. The grid is represented Figure 6.2-a.

Figure 6.2-a: Quadratic grid 3D

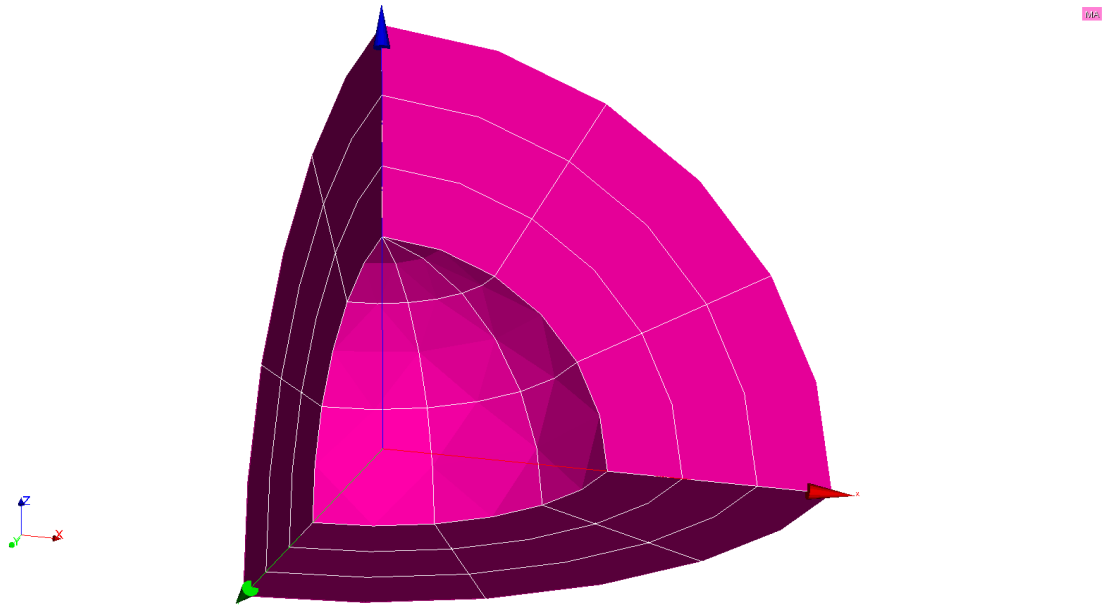

6.3 Sizes tested and results

The results are got with *Code_Aster* (resolution with STAT_NON_LINE). Radial displacements are tested u_r on the lips of the crack. For each crack, it is tested MIN and it MAX of these two sizes for all the nodes of the crack. The got results are synthesized in the table below.

Sizes tested	Type of reference	Analytical values	Tolerance (%)
DR. (int) MIN	'ANALYTICAL'	-0.0001142742582	1.
DR. (int) MAX	'ANALYTICAL'	-0.0001142742582	1.
DR. (ext.) MIN	'ANALYTICAL'	6.173526141E-05	1.
DR. (ext.) MAX	'ANALYTICAL'	6.173526141E-05	1.

Radial displacement u_r and the deformation are represented on the Figure 6.3-a. One observes a clear discontinuity of displacements and the spherical symmetry of the fields.

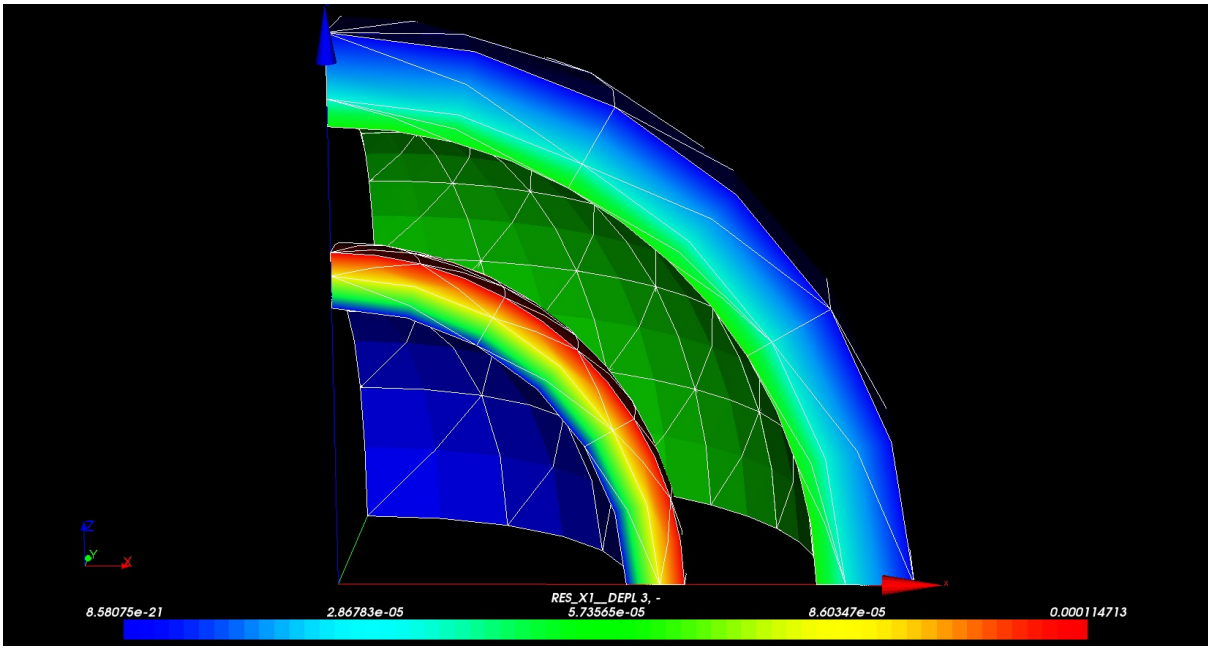

Figure 6.3-a : Field of radial displacement

With the same number of meshs that in preceding modeling, one gets results definitely more precise (one gains a factor 10 in precision on displacements). These two modelings once again illustrate the considerable contribution of the quadratic elements compared to the linear elements. The results got in this last modeling are completely satisfactory, especially taking into consideration the low number of meshs used and curve of the lsn.

7 Conclusion

4 modelings validate the use of the facets of contact resulting from under elements from integration XFEM for the application from mechanical efforts from pressure (normal pressure and shearing in 2D and normal pressure in 3D) on the lips from a crack nonwith a grid. They also illustrate the profit of precision obtained with quadratic elements compared to linear elements.